Adsorption of C_{60} and C_{84} on the Si(100)2×1 surface studied by using the scanning tunneling microscope

X.-D. Wang, T. Hashizume, H. Shinohara,* Y. Saito,† Y. Nishina, and T. Sakurai
Institute for Materials Research, Tohoku University, Sendai 980, Japan
(Received 4 January 1993)

The adsorption of C_{60} and C_{84} on the Si(100)2×1 surface is investigated by using the scanning tunneling microscope (STM) and the scanning tunneling spectroscope (STS). Both of the molecules occupy the trough surrounded by four neighboring dimers. The results show that both C_{60} and C_{84} form strong bonds with the Si substrate. Multiple-layer adsorption of C_{60} and C_{84} results in formation of ordered crystalline islands with the fcc(111) configuration. The internal structures have also been observed for the C_{60} and C_{84} molecules of the first layer adsorbed on the Si(100) surface. In the case of the C_{84} molecules, those of the ordered multiple-layer surface also show similar internal structures. We take these STM images as evidence that the rotation of the individual fullerenes is suppressed significantly on the Si surface. Comparing with the theoretical results, these STM images are attributed to the reflection of the partial charge density of the states of the molecule near the Fermi level. The electronic structures characterized by STS are in good agreement with the recent theoretical calculation and show significant charge transfer from the Si substrate to the adsorbates.

I. INTRODUCTION

The interest in C_{60} (Refs. 1 and 2) has been increasing very rapidly in the last several years. Recently, the successful isolation and extraction of larger fullerenes (C_{70}, C_{76}, C_{84}, C_{90}, C_{96}, etc.) (Refs. 3–6) has made it even possible to extend detailed study to these larger fullerenes. In the last two years, C_{60} adsorbed on Au(111) (Ref. 7) and (110),[8] highly oriented pyrolytic graphite (0001),[9] and GaAs (Ref. 10) surfaces have been investigated by using scanning tunneling microscopy (STM). While those surfaces are thought to be rather inert, it is well known that there is a high density of dangling bonds on the Si(111)7×7 (Ref. 11) and Si(100)2×1 (Ref. 12) surfaces. Therefore, a considerable amount of charge transfer can be expected in the case of fullerene adsorption on these Si surfaces. Furthermore, Si is one of the most important materials in the electronic device industry and semiconductor physics, so that understanding the interaction of C_{60} and other fullerenes with the Si surfaces is especially important. In this paper, we present our recent study on C_{60} and C_{84} adsorption on the Si(100)2×1 surface using the field ion–scanning tunneling microscope (FI–STM).

II. EXPERIMENT

The experimental details of the C_{60} and C_{84} purification,[13–15] deposition,[16] and STM instrumentation[17] have been reported elsewhere and will not be described here in detail. Briefly speaking, our FI–STM is a combination of a high-performance scanning tunneling microscope (STM) and a room-temperature field ion microscope (FIM) which is used for the precise characterization of the scanning tip and its atomic scale fabrication. To obtain needed stability and excellent duty-cycle performance, ⟨111⟩-oriented single-crystal tungsten tips are used. The main UHV chamber is pumped by a 1200 *l*/s custom-design ion pump and the base pressure is below 3×10^{-11} Torr. The pressure rise during the final annealing of the Si sample does not go beyond 1×10^{-10} Torr with this well-designed, fast pumping system. The purity of C_{60} and C_{84} samples is 99.5% and 98%, respectively. The fullerene source is placed inside a small Ta-made dispenser. After degassing the dispenser thoroughly in the UHV chamber, it is brought near the clean Si(100)2×1 surface and heated at proper temperatures, i.e., approximately 330 °C for C_{60} and 400 °C for C_{84}, to evaporate C_{60} and C_{84} molecules.[18,19] The clean Si(100)2×1 surface (Fig. 1) is obtained by repeatedly an-

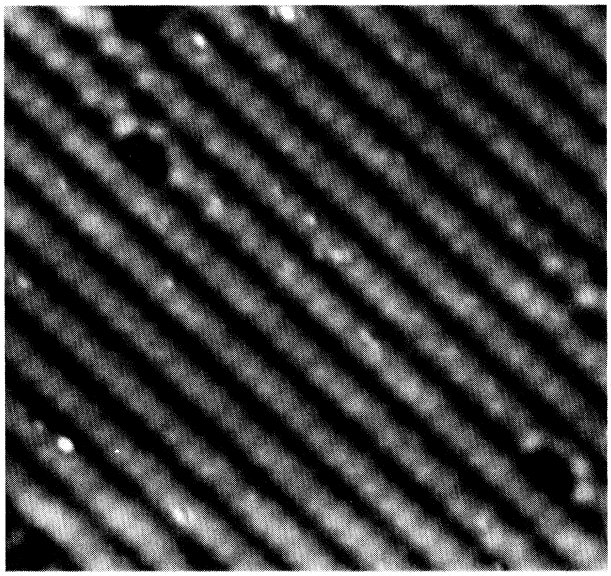

FIG. 1. STM image of the clean Si(100)2×1 surface, showing a very small defect density. (Sample bias $V_s=-1.6$ V, tunneling current $I_t=20$ pA, 92×92 Å^2.)

nealing the Si(100) wafer up to 1220 °C. The defect density is kept at less than 0.1% as shown in Fig. 1, in order to ensure that the fullerene adsorption we have studied is not influenced by the substrate defects.

III. RESULTS AND DISCUSSION

A. C_{60} adsorption on the Si(100)2×1 surface

1. Initial stage

First, we present the initial stage of C_{60} adsorbing on the Si(100)2×1 surface. Figure 2 shows C_{60} molecules adsorbed on the Si(100)2×1 surface with 0.02 monolayers (ML's). C_{60} molecules are imaged as large bright spherical protrusions. When we scan the surface at the sample bias voltage smaller than 1.6 V, we occasionally observed C_{60} molecules being dragged by the tip due to a large band gap of C_{60}, as indicated in the half-split images of the molecules in Fig. 2. It can also be observed that most of the C_{60} molecules are adsorbed in the trough without any preference to the step edges or nucleation into islands at defect sites. This adsorption behavior is quite different from that on Au (Ref. 7) and Cu (Ref. 20) surfaces where strong segregation is noted to the step edge and shows that the C_{60} molecules strongly bond to the Si substrate. The adsorption position is well defined to be the center of four neighboring dimers (*A* in Fig. 4). The nearest-neighbor distance (NND) of molecules under this coverage is found to be 12 Å, which is larger than that (10.0 Å) in the fcc bulk phase.

2. One monolayer

With a further increase in coverage to one monolayer, the C_{60} overlayer shows local ordering, as shown in Fig. 3. The substrate Si dimer lines run in the diagonal direction in this image. The dark regions are bare patches of the Si(100)2×1 surface. Two types of local orderings can be observed in Fig. 3; one is the square type, which is mainly located in the upper part of the image, and the other is the hexagonal-like arrangement which is located in the lower right of the image. Careful examination of the STM images allows us to propose the following adsorption model.

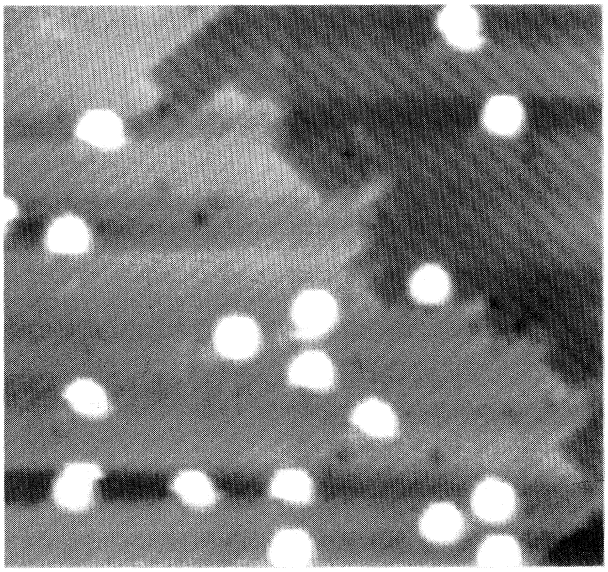

FIG. 2. STM image of the Si(100)2×1 surface adsorbed with approximately 0.02 ML of C_{60} ($V_s=-2.0$ V, $I_t=20$ pA, 270×270 Å^2).

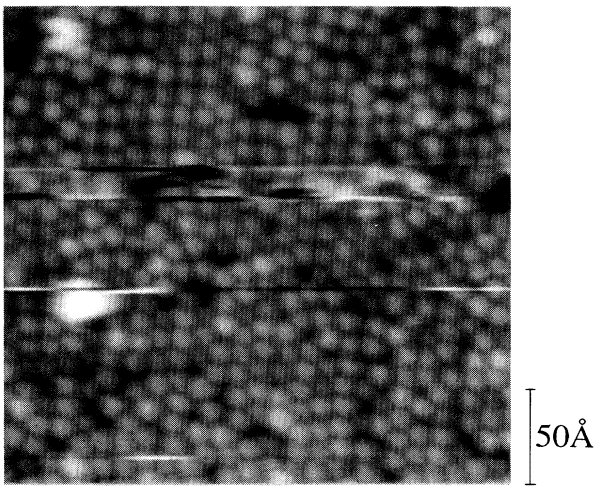

FIG. 3. STM image of the surface with the C_{60} coverage of approximately one monolayer. Square-type ordering with the $c(4\times4)$ configuration can be observed in the upper part of the image while the $c(4\times3)$ quasihexagonal packing is in the lower right of the image. The dark regions are the bare Si surface not covered by C_{60} ($V_s=-4.0$ V, $I_t=20$ pA).

Figure 4 represents the adsorption position and the local ordering based on the STM study. The hatched and solid pairs of circles are the buckled Si dimers where the hatched ones are lower Si atoms and the solid ones are upper atoms. The large open circles are C_{60} molecules. At first, C_{60} resides at position *A*, which is the center of four neighboring Si dimers, surrounded by eight Si atoms. When the coverage slightly increases, the second C_{60} may occupy position *B* [Fig. 4(a)] or *B'* [Fig. 4(b)]. The nearest-neighbor distance at submonolayer coverages is determined to be 12 Å by our STM images, slightly larger than the spacing between *A* and *B* in the schematic which is 10.9 Å. The measured slightly larger NND suggests the presence of the repulsive interaction between neighboring C_{60}'s, due likely to the result of charge transfer from the Si substrate.

From the adsorption positions presented in Fig. 4, the two types of local orderings observed by STM can be derived naturally. The local ordering shown in Fig. 4(a) represents the square-type arrangement: the $c(4\times4)$ overlayer. The nearest-neighbor distance in this case is 10.9 Å. The local arrangement shown in Fig. 4(b) forms a quasihexagonal structure: the $c(4\times3)$ structure. In this geometry, the distance between *A* and *A* is 11.5 Å and the distance between *A* and *B'* is 9.6 Å. The number density of molecules is $1.13\times10^{14}/\text{cm}^2$ and

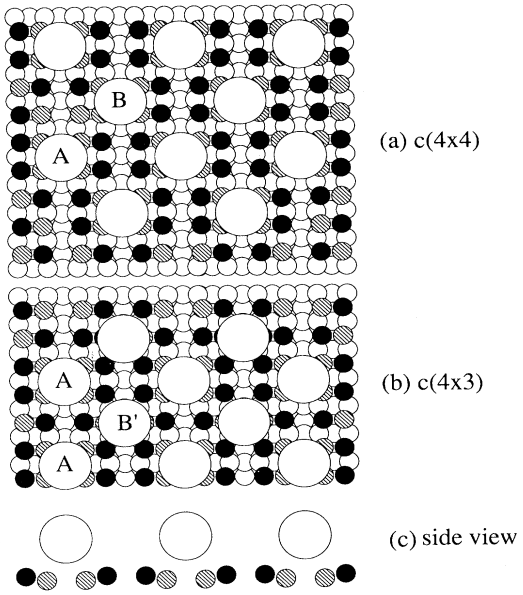

FIG. 4. Schematic of the adsorption position of the first layer of C_{60} on the Si(100)2×1 surface: (a) represents the $c(4\times4)$ configuration, (b) represents the $c(4\times3)$ configuration, and (c) is the side view of (a) and (b) at position A. Small open circles are bulk Si atoms, hatched and solid circles are buckled Si surface dimers with the solid circles representing the upper and the hatched circles representing the lower Si atoms in the dimers. The large open circles are C_{60} molecules.

$8.42\times10^{13}/cm^2$ for the $c(4\times3)$ and $c(4\times4)$ phases, respectively. These values amount to 98% and 73% of that of the fcc(111) surface of the C_{60} crystal($1.15\times10^{14}/cm^2$), respectively. These strained structures of the first layer on the Si(100) surface suggest that the bonding between C_{60} and the Si substrate is much stronger than that among C_{60}'s.

3. *Multiple layer*

With a further increase of the coverage, C_{60} formed multiple-layer islands after completing the first-layer growth as shown in Fig. 5, which indicates that the growth of C_{60} on the Si(100) surface at room temperature is in the Stranski-Krastanov mode. The prominent ordered structure on these islands is the close-packed structure, which is the fcc(111) surface. The ordered structure starts to form above the third layer under the present conditions, as shown in Fig. 6(a), which shows a five-layer island. The first layer and second layer in this image are still somewhat disordered. But from the third layer up to the fifth layer, the formation of the well-ordered hexagonal packing can be observed.

Figure 6(b) is its close-up view, showing the well-ordered surface. We note that this surface exhibits uniform brightness for all molecules, implying a high degree of order and symmetry. The nearest-neighbor distance is measured to be 10.4 Å in this case, which is still slightly

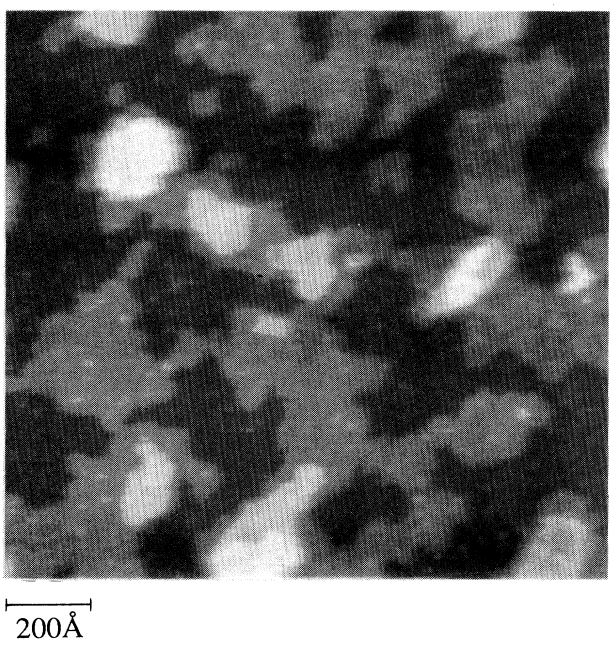

FIG. 5. Large-scale STM image of the C_{60} multiple layers grown on the Si(100)2×1 surface ($V_s=-3.5$ V, $I_t=20$ pA).

larger than the reported value for the bulk (10.0 Å), indicating that the film is not completely relaxed yet. Besides the (111) facet, the (100) facet is also occasionally observed, showing that it is another energetically favorable surface. Several kinds of defects, such as missing-molecular defects and screw dislocations (Fig. 7), as well as their mobile nature are occasionally observed, indicating that the C_{60} surface is quite mobile in the bulk.

4. *Electronic structure*

One of the most important observations we made is that the internal structure can be observed in the first layer of C_{60}. One can see in Fig. 8 that four lines are running parallel in each of the molecules. This kind of structure has never been reported so far by other groups. The previously published results only claimed the observation

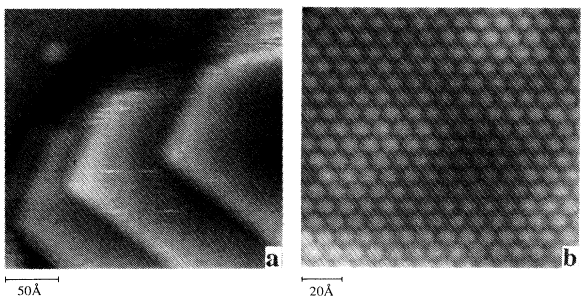

FIG. 6. (a) STM image of a five-layer C_{60} island showing the close-packed fcc(111) surface. (b) An enlarged STM image of the top layer of the surface shown in (a), showing uniform brightness of individual molecules ($V_s=-3.5$ V, $I_t=20$ pA).

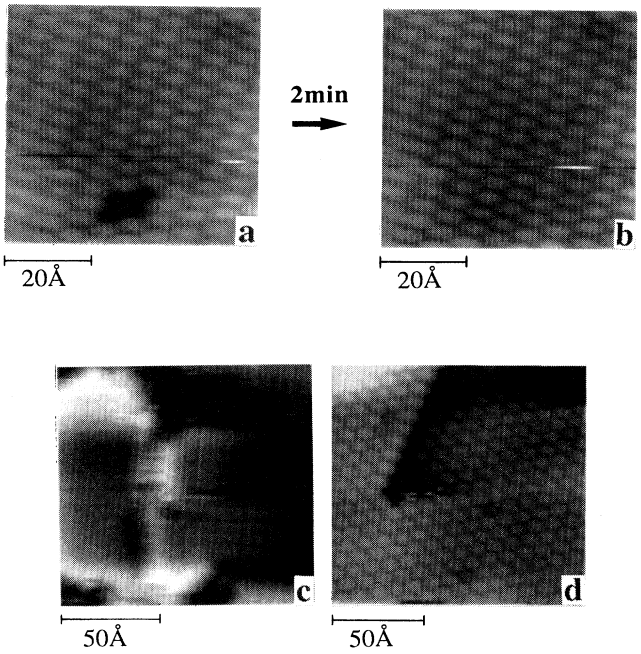

FIG. 7. STM images of several kinds of defects and facets. (a) Four missing-molecule defects at the lower part of the image ($V_s=-4.0$ V, $I_t=20$ pA) and (b) the same area as shown in (a) imaged after 2 min ($V_s=-4.0$ V, $I_t=20$ pA), showing the filling of the missing-molecule defects by other molecules. (c) STM image of the fcc(100) facet at the right side of the (111) facet, noting that the (100) facet is not parallel to the substrate surface ($V_s=-3.5$ V, $I_t=20$ pA). (d) STM image showing a screw dislocation ($V_s=-3.0$ V, $I_t=20$ pA).

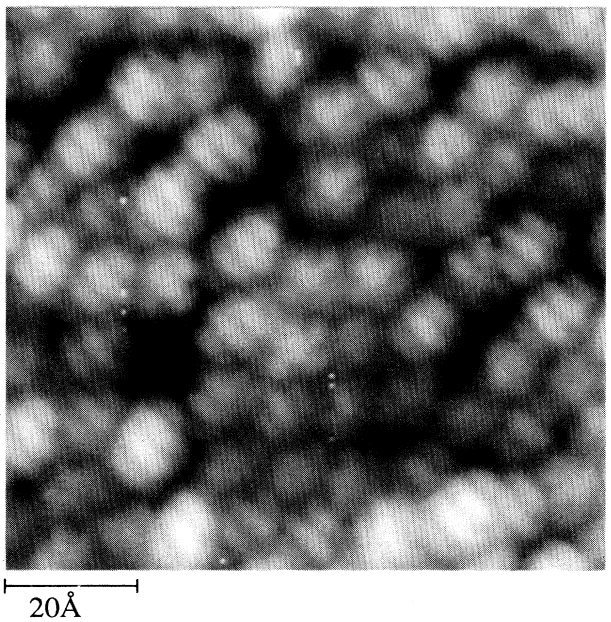

FIG. 8. STM image of the first layer of the C_{60} on the Si(100) surface. The Si dimer rows of the substrate run in the diagonal direction. The image shows some internal structures (mainly four stripes running in parallel), reflecting the partial density of states near the Fermi level.

of either hexagonal or pentagonal rings.[8,21] However, a recent theoretical calculation of the charge-density distribution of Kawazoe's group[22] supports our STM data. Figure 9 shows the calculated distributions of the electronic density states of the C_{60} molecule on the Si(100)2×1 surface with the $c(4\times3)$ configuration.[22] It can be clearly seen that the charge-density distributions of the lowest unoccupied molecular orbital (LUMO) and highest occupied molecular orbital (HOMO) bands do exhibit stripes similar to our STM images. Our STM image is reflecting the local electronic density states near the Fermi level, mainly, of the LUMO and HOMO states.

In order to further characterize the electronic struc-

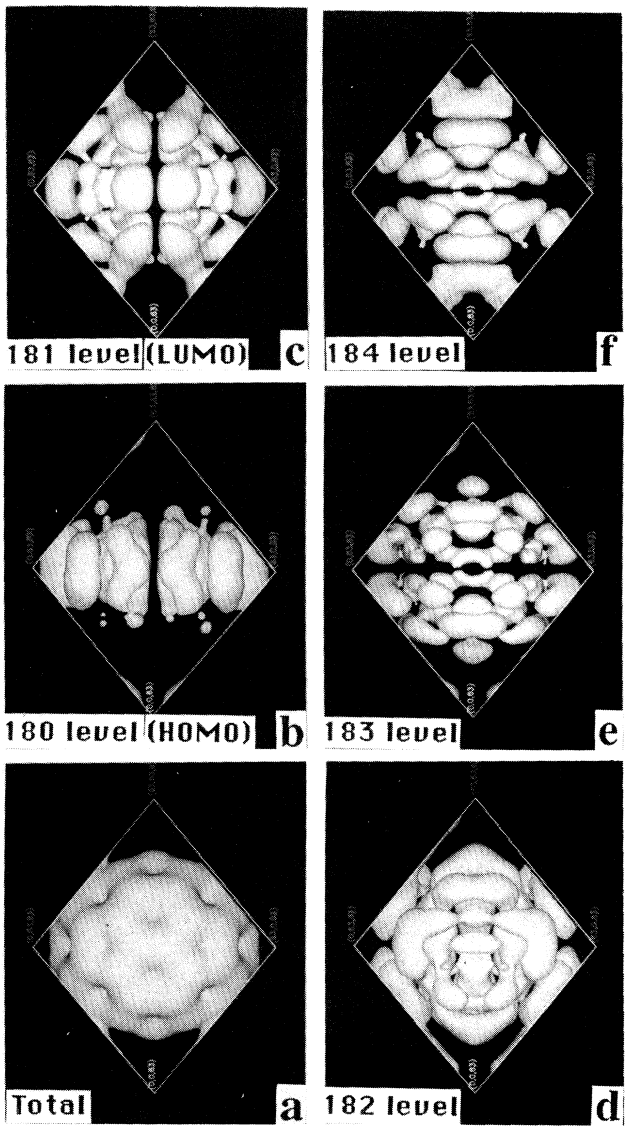

FIG. 9. Calculated charge-density distribution of a C_{60} molecule in the $c(4\times3)$ phase on the Si(100)2×1 surface (Ref. 22). (a) Total charge density, (b) the 180th level charge density, which is the HOMO band, (c) the 181st level charge density, which is the LUMO band, (d) the 182nd level charge density, (e) the 183rd level charge density, and (f) the 184th level charge density.

ture, scanning tunneling spectroscopy (STS) measurements have been performed. Figure 10(a) shows the density of the electronic structure of the first layer of the undoped C_{60} on the Si(100)2×1 surface. The solid curve is the experimental result and the dashed curve is the density of states calculated by Kawazoe and Ohno,[23] where energy zero is taken at the Fermi level. Figure 10(a) shows quite a good agreement between the experiment and calculated results, even though considerable differences are noted between our results and the electronic structures of the bulk C_{60} fcc crystal obtained by photoemission spectroscopy,[24,25] inverse photoemission spectroscopy,[26] and also by several other calculations.[27,28] For example, the measured band gap in our experimental results is approximately 0.9 eV. This is quite smaller than that (1.6 eV) for the fcc crystal.[27] The differences in the electronic structures can be attributed possibly to the difference between the lattice parameters of C_{60} on the Si(100) surface and in the bulk fcc crystal, instead of the charge transfer from the Si substrate. As has been shown, the density of the C_{60} molecule on the Si(100) surface is $8.42\times10^{13}/cm^2$ for the $c(4\times4)$ phase, much smaller than that of the C_{60} bulk. So it can be concluded that the strong bonding to the Si substrate which produces the observed ordering of the C_{60} layer may significantly influence the electronic structure.

Furthermore, our experimental results show that the Fermi level is shifted towards the LUMO band due to the charge transfer from the Si substrate, as shown in Fig. 10(a). This results in the metallic feature of the surface. However, the charge transfer does not appear to cause noticeable changes in the band structure itself. A similar observation is made upon K doping [Fig. 10(b)]. Figure 10(b) is obtained after potassium doping of the C_{60} layer with the ratio of K to C_{60} approximately to unity. It shows that the Fermi level shifts higher by 0.5 eV due to the electron donation from K. However, the band structure itself remains unchanged, consistent with the calculation.[23] A detailed study of the electronic structure of undoped and K-doped C_{60} layers on the Si(100) surface is in progress and will be published elsewhere.

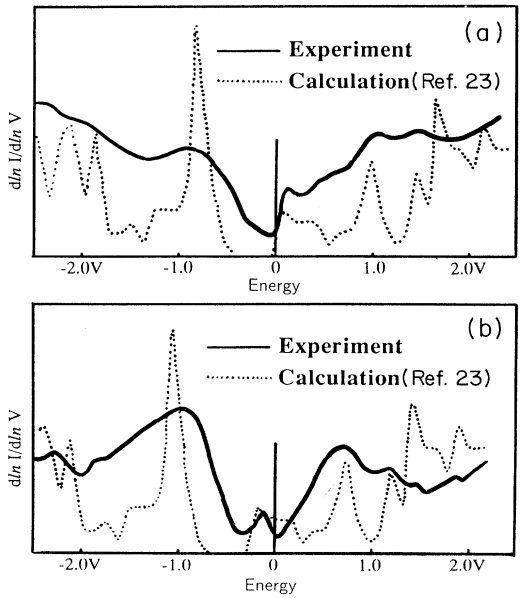

FIG. 10. Scanning tunneling spectroscopy (solid curves) of the (a) first layer of C_{60} on the Si(100)2×1 surface, and (b) K-doped C_{60} layer on the Si(100)2×1 surface; the ratio of K to C_{60} is approximately one. The dashed curves are the calculated density of states (Ref. 23). The energy is referred to the Fermi level.

B. C_{84} adsorption on the Si(100)2×1 surface

The C_{84} molecules are imaged significantly larger than C_{60} in the STM image. Their diameter is approximately 10% larger than that of C_{60}. The C_{84} molecules in the first layer are strongly bonded to the Si(100)2×1 surface, mostly at the trough between dimer rows, and distribute randomly on the surface without preference to the step edge or nucleating into islands, similar to the case of C_{60}. The minimum separation is 14 Å when the C_{84} number density is small. However, the local ordering is less evident, as shown in Fig. 11, because of the larger misfit between the size of C_{84} and the Si(100)2×1 unit size.

Furthermore, we have found that the ordered structure cannot be observed for the multiple-layer adsorption of C_{84} when the substrate is kept at room temperature during C_{84} deposition. The C_{84} crystalline islands are successfully formed, only when the substrate is heated at approximately 100–150 °C during the deposition. Figure 12(a) shows a C_{84} crystalline island, which is about 3000 Å in size. The close-up view of the ordered structure on this island is shown in Fig. 12(b), detailing the hexagonal lattice structure. To our knowledge, this is the first time the crystal structure of C_{84} is observed by the STM. The nearest-neighbor distance is determined to be 12.1±0.2 Å.

One important and interesting observation of the ordered structure is that the individual C_{84} molecules are

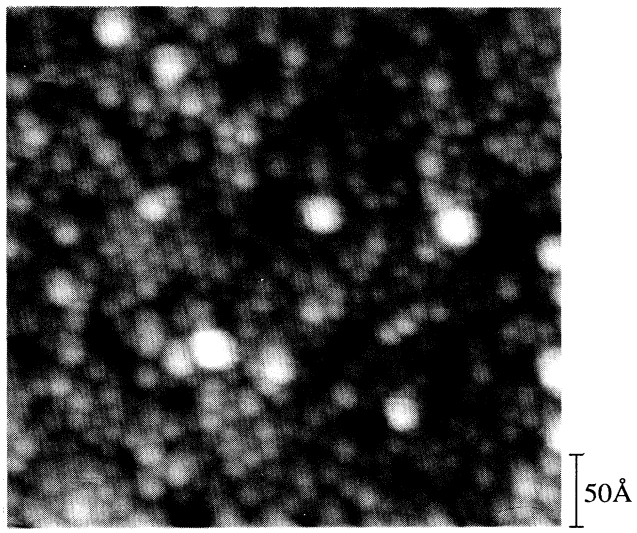

FIG. 11. The first layer of C_{84} on the Si(100)2×1 surface ($V_s=-4.0$ V, $I_t=50$ pA).

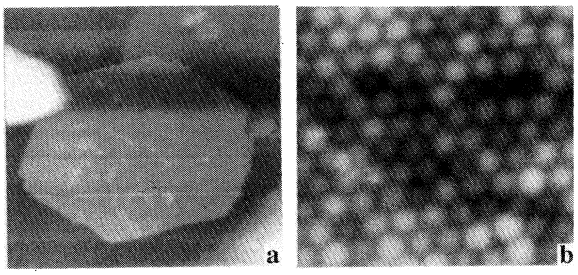

FIG. 12. (a) A large-scale STM image of a crystalline island ($V_s=-4.0$ V, $I_t=50$ pA, 3650×4000 Å^2). (b) A close-up view of the ordered structure ($V_s=-4.0$ V, $I_t=50$ pA, 120×120 Å^2).

not imaged uniformly in image brightness, unlike the case of the ordered C_{60} surface on the Si(100) surface (Fig. 6). The height difference between the highest and lowest imaged molecules is approximately 1.2 Å. This observation suggests that there are several types of stable C_{84} isomers stably coexisting on the Si(100) surface, and they are not completely spherical. In fact, direct computer searching of structures by Manolopoulos and Fowler[29] has derived 24 possible isomers of C_{84}. NMR results[30] have revealed that the isolated C_{84} sample consists of two isomers. One is the D_{2d} structure, which is model no. 23 in Fig. 4 of Ref. 29. Another one is one of the four isomers with D_2 symmetry presented in Ref. 29. However, since there are four candidates for D_2, the determination of the existing D_2 isomer is still in controversy. The D_2 (no. 5) model proposed by Wakabayashi and Achiba[31] according to their ring stacking growth model, is supported by the calculations of Saito and co-workers[32,33] using the local-density approximation, while the calculation by Wang *et al.*[34] using the first-principles calculation and Raghavachari[35] using the modified neglect of differential overlap method supports the D_2 (no. 22) structure which is the lowest in energy. Saito *et al.*[33] also calculated the size of four C_{84} isomers with the D_2 symmetry in three twofold axes. The results show that the maximum and minimum diameters for D_2 (no. 5) are 9.38 and 6.53 Å, respectively, which is almost a 3-Å difference, while the D_2 (no. 22) is rather spherical, the difference in the maximum and minimum diameters being only 0.7 Å. Our STM observation of the ordered C_{84} surface shows only approximately 1.2 Å in height difference. Our preliminary statistical analysis of the individual C_{84} molecules on the Si(100)2×1 surface shows less than a 10% difference between the maximum and minimum diameters and the height is calibrated to be less than 8.6 Å, assuring that the height of C_{60} on the same surface is 7.1 Å.[18] We, therefore, suggest that the no. 22 isomer proposed by Ref. 34 is the most preferred C_{84} isomer with the D_2 symmetry.

Figure 13 is the STM image of C_{84} showing the crystalline island with the hexagonal packing face (lower left) together with the square packing face (upper right). The surface with the square structure is faceted by 25° with respect to the hexagonal domain. This STM image clearly shows, considering the relationship between these two

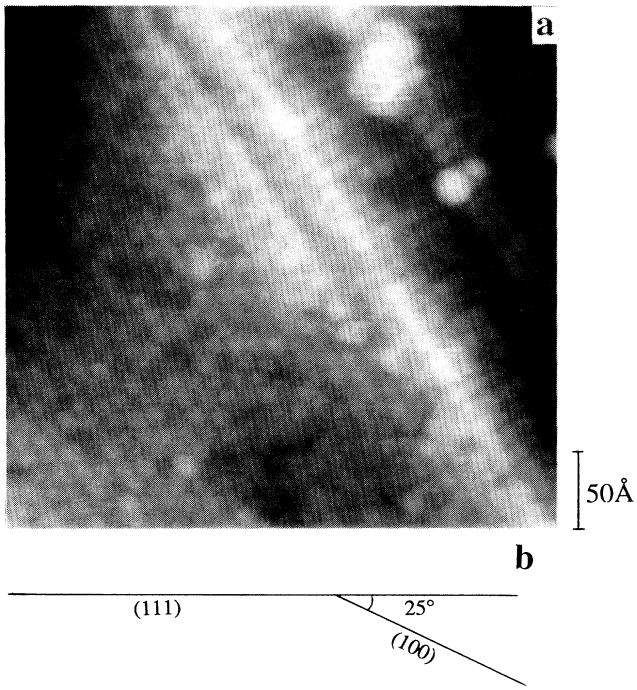

FIG. 13. (a) STM image showing an ordered crystalline island with the hexagonal arrangement face together with the square arrangement facet ($V_s=-4.0$ V, $I_t=50$ pA). (b) The schematic of the cross section of the two faces showing the angle between these two facets to be 25°.

domains, that the C_{84} molecules form the fcc structure in the solid phase, instead of the hcp structure.

In contrast to the case of C_{60}, the internal structures of C_{84} are observed also at the surface of the crystalline island, as shown in Fig. 14. We can see that stripes as well

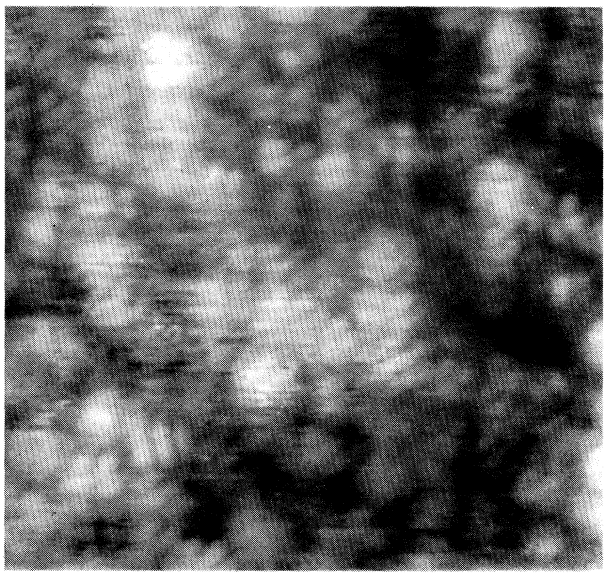

FIG. 14. STM image of the ordered layer of C_{84} revealing the internal structures, which indicates the C_{84} molecules in crystal remain fixed without rotation ($V_s=-2.5$ V, $I_t=50$ pA, 120×120 Å^2).

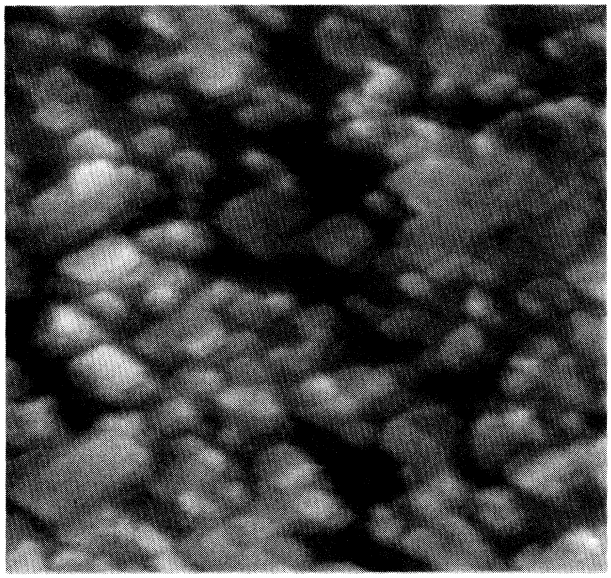

FIG. 15. Large-scale STM image of SiC islands after annealing the C_{84} layer on the Si(100)2×1 surface at 1000 °C ($V_s = -2.5$ V, $I_t = 50$ pA, 2000×2700 Å^2).

as several spots are imaged in individual molecules. Even though the atomic arrangement of C_{84} cannot be derived from this image, it implies that the C_{84} may remain fixed in crystal without rotation. The orientation is somehow disordered, indicating that the cohesive energy among C_{84} molecules is different, depending on the molecular orientation. Since the desorption temperature naturally increases with increasing mass of fullerenes,[36,37] internal rotation of larger fullerenes may stop at room temperature.

A preliminary study is performed on the desorption of C_{84} layers by heating the multiple-layer adsorbed C_{84} surface successively up to 1300 °C. The desorption of C_{84} multiple layers above the first layer occurs easily at approximately 400 °C. However, the first layer is surprisingly stable upon annealing until the temperature exceeds 1000 °C. Above 1000 °C, reactions with the Si substrate occur, resulting in the formation of silicon carbide islands on the surface (Fig. 15). A similar phenomenon was also observed in the case of C_{60} adsorption on the Si(100) surface. The detailed discussion on the silicide formation will be reported later.

IV. CONCLUSIONS

Our STM results show the following.

1. Both C_{60} and C_{84} molecules bond strongly to the Si(100) surface without any preference to the step edge or nucleation at the defects in the first layer. The adsorption position has been determined to be the trough between dimer rows.

2. Multiple-layer islands are formed for both C_{60} and C_{84} after completing the first layer. A well-ordered fcc(111) phase structure could be observed on these islands. The fcc(100) facet is also observed occasionally.

3. The electronic structures of the undoped and K-doped C_{60} layers are measured using STS and compared with theoretical calculations.

4. The internal structures of C_{60} and C_{84} in the first layer are observed, reflecting the partial charge-density distribution in the molecules. This is taken as evidence that the rotation of the molecules stops on the Si(100)2×1 surface. In contrast to the case of C_{60} in the solid phase, the C_{84}'s in multiple-layer islands are not rotating at room temperature.

5. The crystal structure of C_{84} is the fcc.

6. The no. 22 isomer of Ref. 29 is the most preferred C_{84} isomer with the D_2 symmetry among four possible candidates.

7. The multiple layers of C_{60} and C_{84} can be desorbed by heating the sample at modest temperatures. However, the first layers of C_{60} and C_{84} can never be desorbed. They appear to react with the Si surface at temperatures above 1000 °C, forming the SiC layer.

*Permanent address: Department of Chemistry for Materials, Faculty of Engineering, Mie University, Tsu, Mie 514, Japan.
†Permanent address: Department of Electrical Engineering, Faculty of Engineering, Mie University, Tsu, Mie 514, Japan.

[1]H. R. Kroto, J. R. Heath, S. C. O'Brien, R. F. Curl, and R. E. Smalley, Nature **318**, 162 (1985); R. F. Curl and R. E. Smalley, Sci. Am. **265**, 32 (1991).
[2]W. Krätschmer, K. Fostiropoulos, and D. R. Huffman, Chem. Phys. Lett. **170**, 167 (1990); W. Krätschmer, L. D. Lamb, K. Fostiropoulos, and D. R. Huffman, Nature **347**, 354 (1990).
[3]K. Kikuchi, N. Nakahara, T. Wakabayashi, M. Honda, H. Matsumiya, T. Moriwaki, S. Suzuki, H. Shiromaru, K. Saito, K. Yamakuchi, I. Ikemoto, and Y. Achiba, Chem. Phys. Lett. **188**, 177 (1992).
[4]F. Diederich, R. L. Whetten, C. Thilgen, R. Ettl, I. Chao, and M. M. Alvarez, Science **254**, 1768 (1991).
[5]F. Diederich, R. Ettl, Y. Rubin, R. L. Whetten, R. Beck, M. Alvarez, S. Anz, D. Sensharma, F. Wudl, K. C. Khemani, and A. Koch, Science **252**, 548 (1991).
[6]H. Shinohara, H. Sato, Y. Saito, A. Izuoka, T. Sugawara, H. Ito, T. Sakurai, and T. Matsuo, Rapid Commun. Mass Spectrom. **6**, 413 (1992).
[7]E. I. Altman and R. J. Colton, Surf. Sci. **279**, 49 (1992); L. D. Lamb, D. R. Huffman, R. K. Workman, S. Howells, T. Chen, D. Sarid, and R. F. Ziolo, Science **255**, 1413 (1992); T. Chen, S. Howells, M. Gallagher, L. Yi, D. Sarid, D. L. Lichtenberger, K. W. Nebesny, and C. D. Ray, J. Vac. Sci. Technol. B **10**, 170 (1992); R. J. Wilson, G. Meijer, D. S. Bethune, R. D. Johnson, D. D. Chambliss, M. S. de Vries, H. E. Hunziker, and H. R. Wendt, Nature **348**, 621 (1990).
[8]Y. Zhang, X. Gao, and M. J. Weaver, J. Phys. Chem. **96**, 510 (1992).
[9]J. L. Wragg, J. E. Chamberlain, H. W. White, W. Krätschmer, and D. R. Huffman, Nature **348**, 623 (1990).
[10]Y. Z. Li, J. C. Patrin, M. Chander, J. H. Weaver, L. P. F. Chibante, and R. E. Smalley, Science **252**, 547 (1991); Y. Z. Li,

M. Chander, J. C. Patrin, J. H. Weaver, L. P. F. Chibante, and R. E. Smalley, *ibid.* **253**, 429 (1991).
[11]K. Takayanagi, Y. Tanishiro, M. Takahashi, and S. Takahashi, J. Vac. Sci. Technol. A **3**, 1502 (1985).
[12]R. J. Hamers, R. M. Tromp, and J. E. Demuth, Phys. Rev. Lett. **56**, 1972 (1986).
[13]H. Shinohara, H. Sato, Y. Sato, M. Takayama, A. Izuoka, and T. Sugawara, J. Phys. Chem. **95**, 8449 (1991).
[14]Y. Saito, K. Kurosawa, H. Shinohara, S. Saito, A. Oshiyama, Y. Ando, and T. Noda, J. Phys. Soc. Jpn. **60**, 2518 (1991).
[15]Y. Saito, N. Suzuki, H. Shinohara, and Y. Ando, Jpn. J. Appl. Phys. **30**, 2857 (1991).
[16]T. Hashizume, X.-D. Wang, Y. Nishina, H. Shinohara, Y. Saito, Y. Kuk, and T. Sakurai, Jpn. J. Appl. Phys. **31**, L880 (1992).
[17]T. Sakurai, T. Hashizume, I. Kamiya, Y. Hasegawa, N. Sano, H. W. Pickering, and A. Sakai, Prog. Surf. Sci. **33**, 3 (1990); T. Hashizume, I. Sumita, Y. Murata, S. Hyodo, and T. Sakurai, J. Vac. Sci. Technol. A **9**, 742 (1991).
[18]X.-D. Wang, T. Hashizume, H. Shinohara, Y. Saito, Y. Nishina, and T. Sakurai, Jpn. J. Appl. Phys. **31**, L983 (1992).
[19]T. Hashizume, X.-D. Wang, Y. Nishina, H. Shinohara, Y. Saito, and T. Sakurai, Jpn. J. Appl. Phys. **32**, L132 (1993).
[20]K. Motai, T. Hashizume, H. Shinohara, and T. Sakurai, Jpn. J. Appl. Phys. **32**, L450 (1993).
[21]S. Howells, T. Chen, M. Gallagher, D. Sarid, D. L. Lichtenberger, L. L. Wright, C. D. Ray, D. R. Huffman, and L. D. Lamb, Surf. Sci. **274**, 141 (1992).
[22]Y. Kawazoe, H. Kamiyama, Y. Maruyama, and K. Ohno, Jpn. J. Appl. Phys. **32**, 1433 (1993); K. Ohno, H. Kamiyama, Y. Maruyama, Y. Kawazoe, Y. Nishina, and K. Shindo, in *Proceedings of the 21st International Conference on the Physics of Semiconductors,* edited by Xide Xie, K. Huang, and L. L. Chang (World Scientific, Singapore, 1992), Vol. 1, p. 489.
[23]Y. Kawazoe and K. Ohno (private communication).
[24]G. K. Wertheim, J. E. Rowe, D. N. E. Buchanan, E. E. Chaban, A. F. Hebard, A. R. Kortan, A. V. Makhija, and R. C. Haddon, Science **252**, 1419 (1991).
[25]J. H. Weaver, J. L. Martins, T. Komeda, Y. Chen, T. R. Ohno, G. H. Kroll, N. Troullier, R. E. Haufler, and R. E. Smalley, Phys. Rev. Lett. **66**, 1741 (1991).
[26]T. Takahashi, S. Suzuki, T. Morikawa, and H. Katayama-Yoshida, Phys. Rev. Lett. **68**, 1232 (1992).
[27]S. Saito and A. Oshiyama, Phys. Rev. Lett. **66**, 2637 (1991).
[28]W. Y. Ching, M.-Z. Huang, and Y.-N. Xu, Phys. Rev. Lett. **67**, 2045 (1991).
[29]D. E. Manolopoulos and P. W. Fowler, J. Phys. Chem. **96**, 7603 (1992).
[30]K. Kikuchi, N. Nakahara, T. Wakabayashi, S. Suzuki, H. Shiromaru, Y. Miyake, K. Saito, I. Ikemoto, M. Kainosho, and Y. Achiba, Nature **357**, 142 (1992).
[31]T. Wakabayashi and Y. Achiba, Chem. Phys. Lett. **190**, 465 (1992).
[32]S. Saito, S. Sawada, and N. Hamada, Phys. Rev. B **45**, 13 845 (1992).
[33]S. Saito, S. Sawada, N. Hamada, and A. Oshiyama (unpublished).
[34]X.-Q. Wang, C. Z. Wang, B. L. Zhang, and K. M. Ho, Phys. Rev. Lett. **69**, 69 (1992).
[35]K. Raghavachari, Chem. Phys. Lett. **190**, 397 (1992).
[36]C. Pan, M. P. Sampson, Y. Chai, R. H. Hauge, and J. L. Margrave, J. Phys. Chem. **95**, 2944 (1991).
[37]H. Shinohara (private communication).

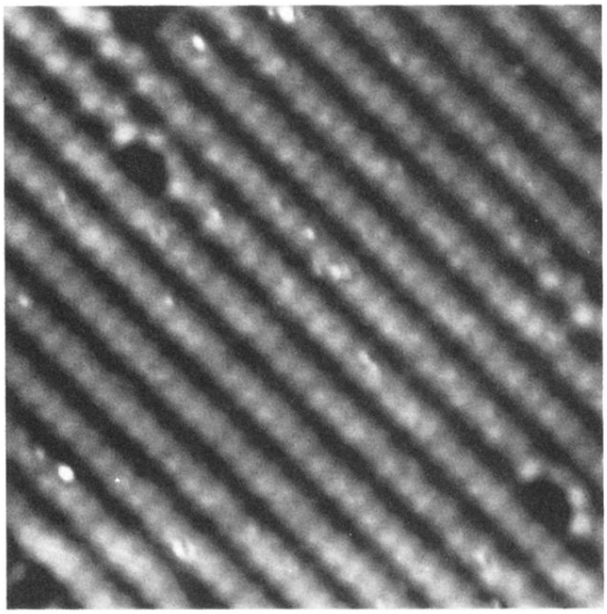

FIG. 1. STM image of the clean Si(100)2×1 surface, showing a very small defect density. (Sample bias $V_s = -1.6$ V, tunneling current $I_t = 20$ pA, 92×92 Å^2.)

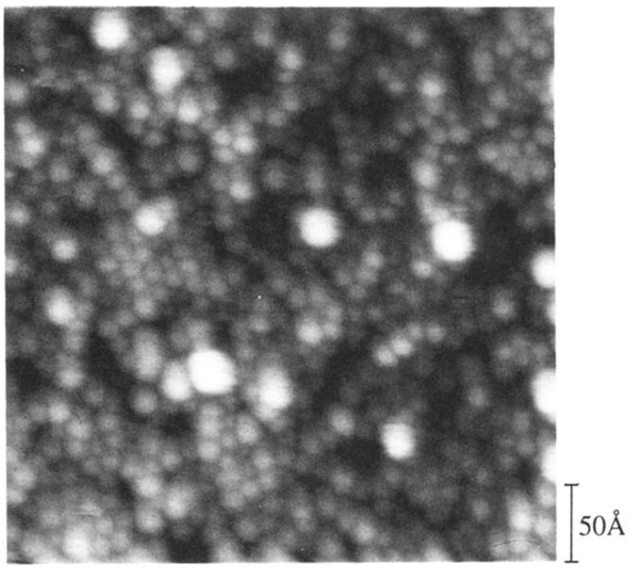

FIG. 11. The first layer of C_{84} on the Si(100)2×1 surface ($V_s = -4.0$ V, $I_t = 50$ pA).

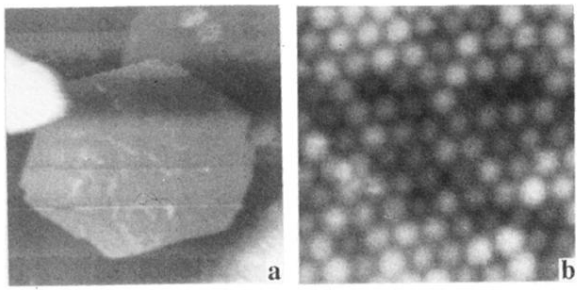

FIG. 12. (a) A large-scale STM image of a crystalline island ($V_s = -4.0$ V, $I_t = 50$ pA, 3650×4000 Å^2). (b) A close-up view of the ordered structure ($V_s = -4.0$ V, $I_t = 50$ pA, 120×120 Å^2).

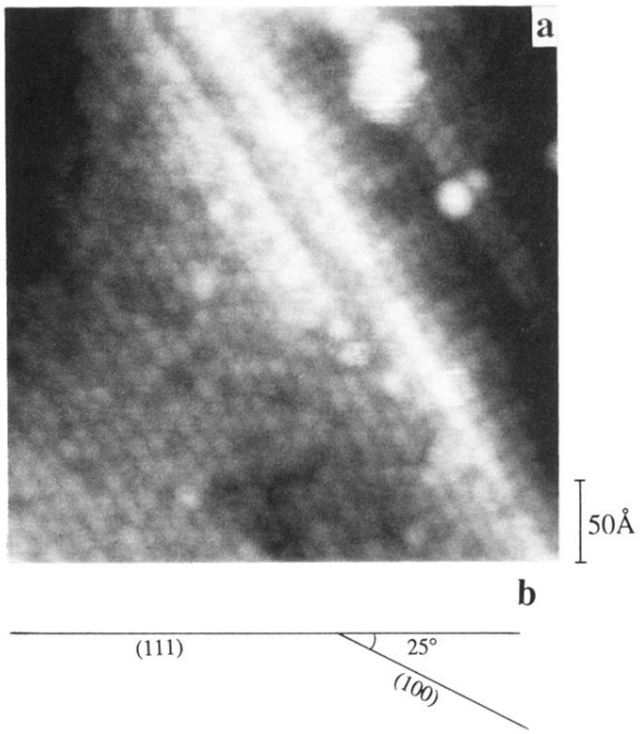

FIG. 13. (a) STM image showing an ordered crystalline island with the hexagonal arrangement face together with the square arrangement facet ($V_s = -4.0$ V, $I_t = 50$ pA). (b) The schematic of the cross section of the two faces showing the angle between these two facets to be 25°.

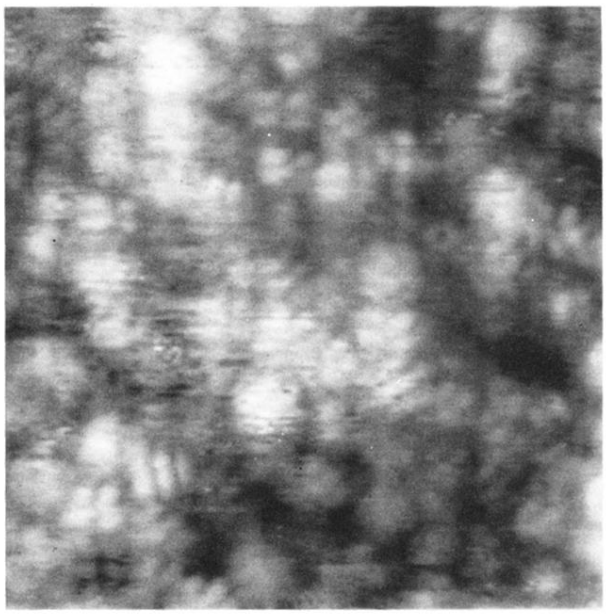

FIG. 14. STM image of the ordered layer of C_{84} revealing the internal structures, which indicates the C_{84} molecules in crystal remain fixed without rotation ($V_s = -2.5$ V, $I_t = 50$ pA, 120×120 Å^2).

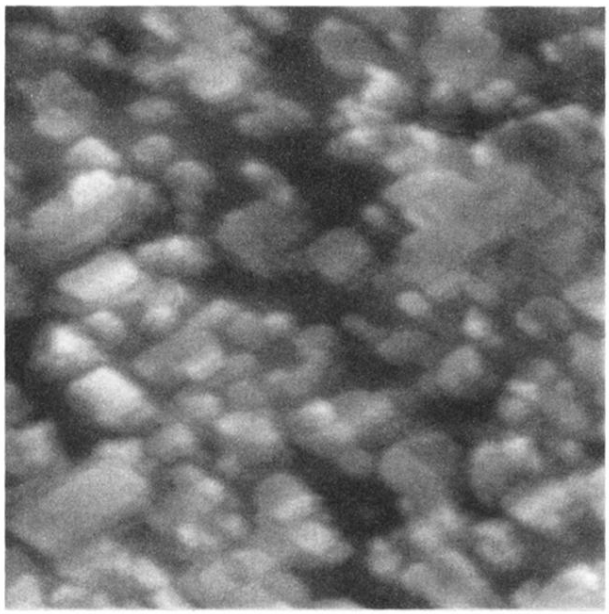

FIG. 15. Large-scale STM image of SiC islands after annealing the C_{84} layer on the Si(100)2×1 surface at 1000 °C ($V_s = -2.5$ V, $I_t = 50$ pA, 2000×2700 Å^2).

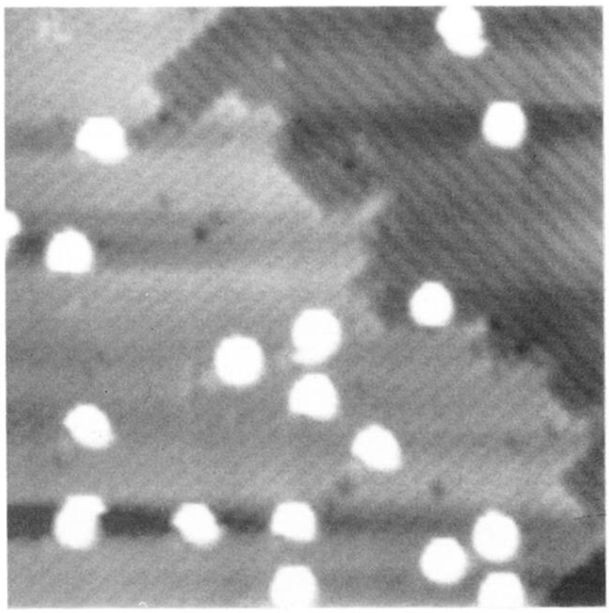

FIG. 2. STM image of the Si(100)2×1 surface adsorbed with approximately 0.02 ML of C_{60} ($V_s = -2.0$ V, $I_t = 20$ pA, 270×270 Å^2).

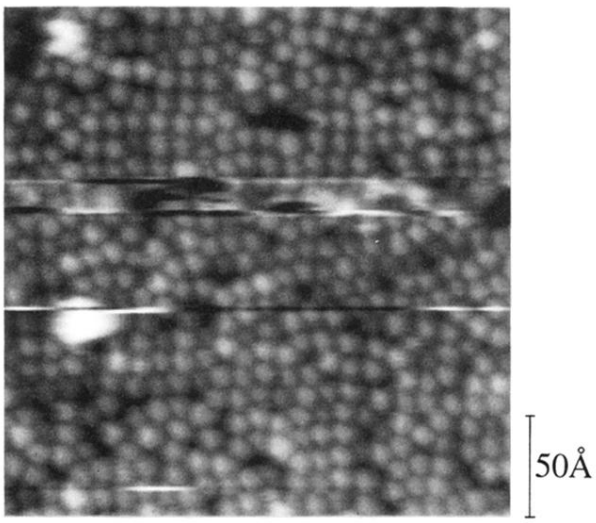

FIG. 3. STM image of the surface with the C_{60} coverage of approximately one monolayer. Square-type ordering with the $c(4\times4)$ configuration can be observed in the upper part of the image while the $c(4\times3)$ quasihexagonal packing is in the lower right of the image. The dark regions are the bare Si surface not covered by C_{60} ($V_s=-4.0$ V, $I_t=20$ pA).

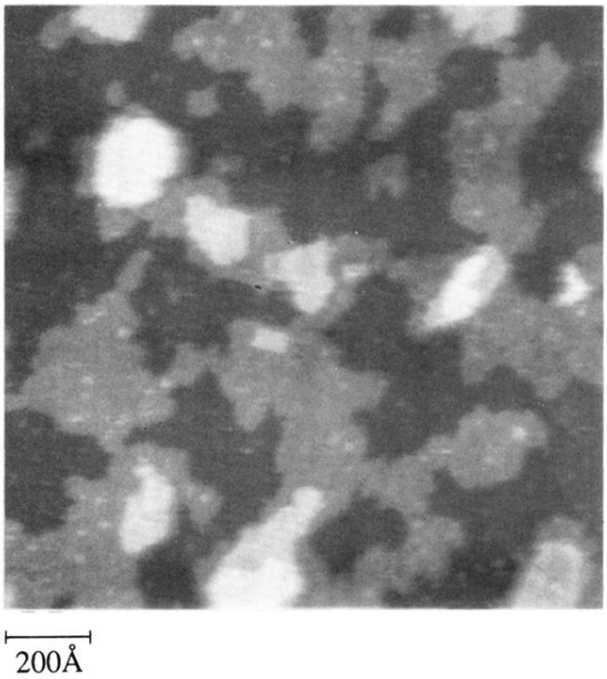

FIG. 5. Large-scale STM image of the C_{60} multiple layers grown on the Si(100)2×1 surface ($V_s = -3.5$ V, $I_t = 20$ pA).

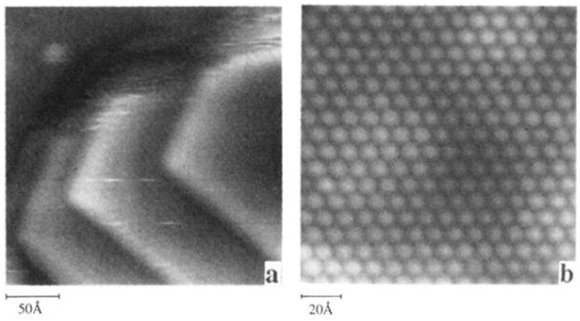

FIG. 6. (a) STM image of a five-layer C_{60} island showing the close-packed fcc(111) surface. (b) An enlarged STM image of the top layer of the surface shown in (a), showing uniform brightness of individual molecules ($V_s = -3.5$ V, $I_t = 20$ pA).

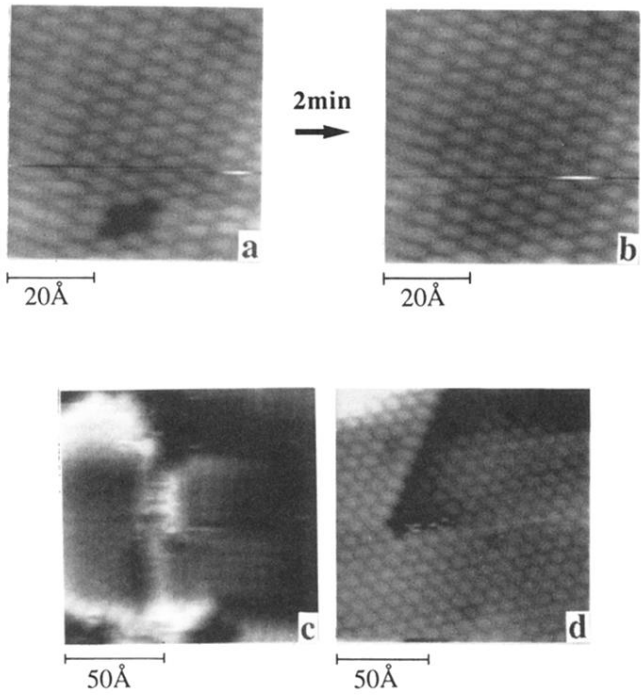

FIG. 7. STM images of several kinds of defects and facets. (a) Four missing-molecule defects at the lower part of the image ($V_s = -4.0$ V, $I_t = 20$ pA) and (b) the same area as shown in (a) imaged after 2 min ($V_s = -4.0$ V, $I_t = 20$ pA), showing the filling of the missing-molecule defects by other molecules. (c) STM image of the fcc(100) facet at the right side of the (111) facet, noting that the (100) facet is not parallel to the substrate surface ($V_s = -3.5$ V, $I_t = 20$ pA). (d) STM image showing a screw dislocation ($V_s = -3.0$ V, $I_t = 20$ pA).

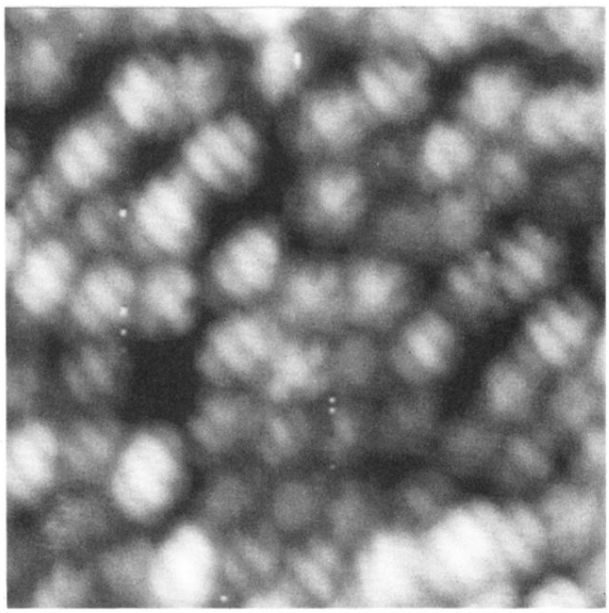

FIG. 8. STM image of the first layer of the C_{60} on the Si(100) surface. The Si dimer rows of the substrate run in the diagonal direction. The image shows some internal structures (mainly four stripes running in parallel), reflecting the partial density of states near the Fermi level.

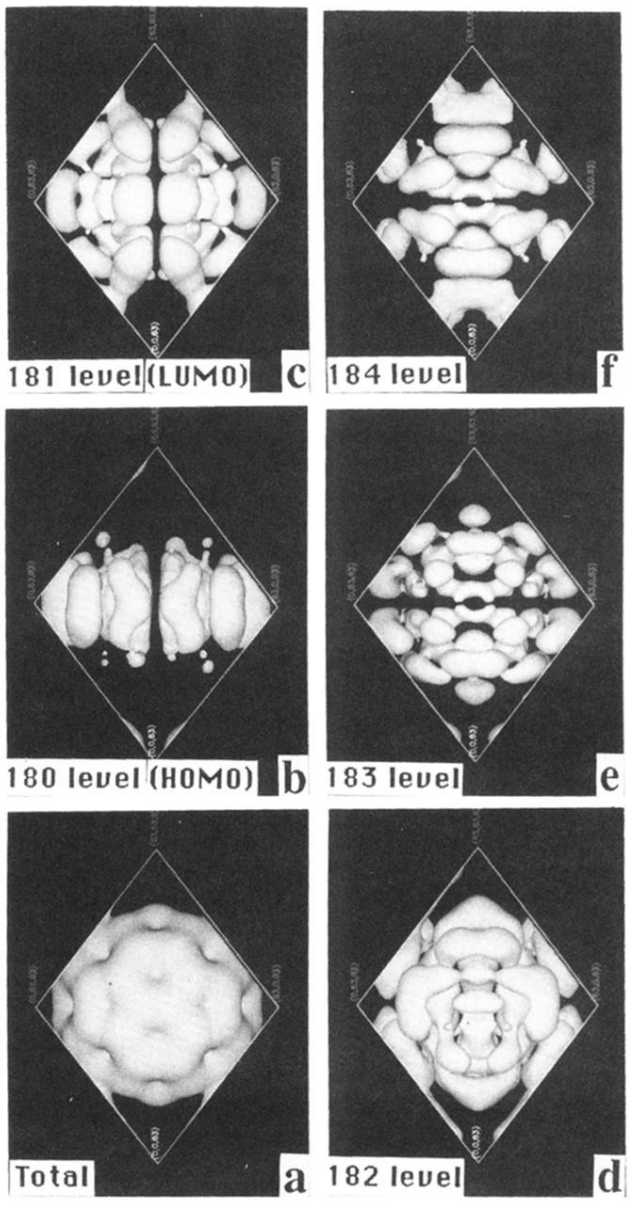

FIG. 9. Calculated charge-density distribution of a C_{60} molecule in the $c(4\times3)$ phase on the Si(100)2×1 surface (Ref. 22). (a) Total charge density, (b) the 180th level charge density, which is the HOMO band, (c) the 181st level charge density, which is the LUMO band, (d) the 182nd level charge density, (e) the 183rd level charge density, and (f) the 184th level charge density.